ISSN-L 2664-9969; E-ISSN 2706-5448

UDC 620.173:622.02
DOI: 10.15587/2706-5448.2025.333869

**Oleksandr Tkachuk,
Daria Chepiga,
Leonid Bachurin,
Serhii Podkopaiev,
Yaroslava Bachurina,
Yevgen Podkopayev,
Mykola Rudynets,
Olena Visyn**

# ASSESSMENT OF DEFORMATION PROCESSES IN BACKFILL MASSES USING CRUSHED ROCK MODELS

*The object of the study was the deformation processes in backfill masses made of crushed rock, which are used for roof control in mining panels. The study addressed the issue of preventing sidewall collapses by ensuring the stability of the backfill masses. Deformation processes were investigated using experimental models made of crushed rock that simulated various backfill structures. The study considered uniaxial compression of crushed rock with lateral expansion capability, as well as compressive loading. Uniaxial compression was used to simulate partial backfilling of the gob area, while compressive loading represented complete backfilling. Under loading conditions, a hyperbolic relationship was established between the relative volume change of the backfill material per unit of side rock convergence, $\Delta V_K$ ($m^{-1}$), and the compaction coefficient of crushed rock. This relationship enables the prediction of the material's ultimate settlement. The determining factor in this relationship is the relative deformation of the backfill mass. Under loading of crushed rock and comparable compaction coefficient values, the difference in deformation properties reaches 2.5 to 3 times. This is recorded due to the transformation of shape or change in volume under different compression conditions. It is shown that with an increase in the parameter $\Delta V_K$, the specific potential energy of deformation of the backfill material changes according to a logarithmic relationship. The specific potential energy of deformation is determined by the mechanical properties and compression conditions of the crushed rock.*

*Maximum stability of gob-side retained entries can be ensured through complete backfilling of the gob area, while the expected subsidence of the backfill mass depends on the initial backfill density and the deformation properties of the crushed rock used for filling.*

***Keywords**: backfill mass, deformation, compaction, crushed rock, convergence, safe working conditions.*

*Received: 05.04.2025*
*Received in revised form: 05.06.2025*
*Accepted: 25.06.2025*
*Published: 30.08.2025*



***How to cite***

*Tkachuk, O., Chepiga, D., Bachurin, L., Podkopaiev, S., Bachurina, Y., Podkopayev, Y., Rudynets, M., Visyn, O. (2025). Assessment of deformation processes in backfill masses using crushed rock models. Technology Audit and Production Reserves, 4 (1 (84)), 50–57. https://doi.org/10.15587/2706-5448.2025.333869*

## 1. Introduction

Underground coal mining is characterized by man-made impact on the environment. One of the factors of such impact is the technology of coal mining, with the release of waste rock to the surface. The waste rocks accumulated in the dumps form unclaimed technological resources.

To place solid mining waste in a coal mine, the backfilling of the gob area is used, which is an effective way to manage the mining pressure in the extraction areas. This method allows for partial neutralization of the harmful manifestations of mining pressure in the coal-bearing rock mass caused by the extraction of minerals and ensures the maintenance of mine roadways. The backfilling of the waste rock in the gob area significantly reduces the effects of surface subsidence, engineering structures, and facilities [1]. When carrying out mining operations with the backfilling of the gob area, the problem of waste-free and environmentally safe production is solvable [1, 2].

The accumulation of waste rocks, slags, and tailings creates environmental and economic problems in mining areas. The maintenance of mine waste dumps and tailings requires significant capital and material costs [3]. Therefore, from an environmental and economic point of view, the main factor that stimulates the use of waste rocks from mine dumps and tailings as backfill materials is the reduction of land areas used for the construction of waste storage facilities. Land is released that can be used for agricultural needs. When using waste rocks, the gob area and gob-side retained entries are converted into a landfill for the placement of solid waste. As a result of backfilling the gob area, the movement of the overburden and underlying strata is limited, ensuring stabilization of the rock mass. The backfill material compensates for the stress relief in the coal-bearing rock mass and contributes to the gradual bending of the lateral rocks. Conditions are created around the mine workings that prevent uncontrolled roof collapse and maintain its stability. However, such a geomechanical state is only achieved within a certain range of deformation properties of the backfill material from the waste rocks. Based on this, an important scientific challenge arises: the use of waste rocks as backfill material. Among the key objectives are maintaining the stability of the gob-side retained entries and improving the safety of miners in the coal mine extraction panels by avoiding collapses of surrounding rocks. However, to address this challenge, it is necessary to understand the physical nature of deformation processes in the backfill mass composed of crushed rock and to determine their impact on the stability of the surrounding strata and gob-side retained entries.

When roof control is implemented by backfilling the gob area with rock material, the artificially created backfill mass functions as a supporting structure and affects the evolution of stress-strain parameters of the coal-rock mass [4]. Indeed, the experience of mines with the backfilling of the gob area demonstrates an improvement in the geomechanical conditions around the mine workings. According to industry regulations, the use of full backfilling may eliminate the need for additional mine roadway protection methods [5]. At the same time, certain studies emphasize the importance of considering the lateral deformation of the backfill masses on the stability of the mine workings [6]. Backfill materials, by partially compensating for the extracted coal body, allow limiting the movement of surrounding rock within the gob area of extraction panels in coal mines [7]. The use of waste rocks helps to reduce the volume of transportation of rock mass, as well as mine waste dumps on the surface. However, the main challenges associated with the use of waste rocks for backfilling include the need for additional crushing and the difficulties of placing them within the gob. Furthermore, waste rock is generally characterized by low bearing capacity.

To ensure the stability of gob-side retained entries, it is proposed to use a hardening backfill, with components that may include waste materials from mining operations [8]. When using this method of backfilling the gob area, the issue of preparing multicomponent mixtures and controlling the hardening process of materials has not been resolved to a certain extent.

The mechanism for improving the condition of the surrounding rocks near the workings lies in the interaction between the compacting backfill and the subsiding roof, when the cracks of the fracture zone above the backfill become closed [9]. However, this effect can only be achieved if the backfill mass provides sufficient load-bearing capacity.

To assess the bearing capacity of backfill masses, it is advisable to take into account the deformation modulus of the crushed rock material [10]. It should be noted that the changes in the deformation modulus during the loading process make it possible to estimate both the elastic and residual deformations of the backfill. Approximately equal values of the deformation modulus indicate the repacking process of the source material under compression.

The known advantages of mining technologies that involve backfilling of the gob area are not fully realized in some cases, which requires further study of the deformation processes under varying compression conditions. The assessment of the bearing capacity of artificially created masses composed of crushed rock is based on the study of the deformation characteristics of backfill materials as bearing supports. Scientific research on this issue is important. The application of such findings will allow for improved measures to maintain the stability of gob-side retained entries, as well as ensuring safer working conditions for miners in extraction panels of coal mines by preventing collapses of surrounding rock.

*The aim of the research* is to reveal the specific features of deformation processes in backfill masses composed of crushed rock under loading, as well as to assess the impact of these processes on the bearing capacity of the backfill as a bearing support. This will ensure the stability of gob-side retained entries and work safety in the extraction areas of coal mines by preventing collapses of lateral rocks in the gob area of the coal mass.

To achieve this aim, the following objectives were set:

– to investigate the variation of the specific potential energy of deformation of backfill masses depending on the mechanical properties and compression conditions of the crushed rock;

– to determine the ultimate compaction coefficient and the ultimate relative deformation of the crushed rock under different compression conditions.

## 2. Materials and Methods

*The object of research* is deformation processes in backfill masses composed of crushed rock, which are used to control the state of surrounding rocks within the extraction panel.

The research hypothesis is that despite differences in the stress-strain state under varying compression conditions of the backfill mass, the energy characteristics of deformation and compaction exhibit a similar pattern. This similarity can be used to predict the bearing capacity and behavior of backfill masses under loading. The internal potential energy of crushed rock backfill masses under loading reaches critical levels at which the stress-strain state of the supporting structures is realized. When these levels are exceeded, the backfill material deforms, and the artificially created mass may change its behavior, which affects the safe operation of the gob-side retained entries. Under such conditions, energy indicators of deformation play a significant role, as they define the deformation capacity and bearing capacity of the backfill masses.

Backfill masses composed of crushed rock were modeled under general conditions of partial or full backfilling of the gob area. Accordingly, uniaxial compression of the crushed rock with the possibility of its lateral expansion and compression loading was considered.

Deformation processes in the crushed rock masses were studied under laboratory conditions and evaluated based on the analysis of the backfill mass model behavior. Model parameters were determined considering geometric and force similarity, assuming identity of dimensionless characteristics [11–13].

The internal friction angle of the model material and the natural material are identical and equal to 23°; the Poisson's ratio for both materials is also the same and equals 0.25.

Geometric similarity is ensured by a single scale ratio relating the sizes of model samples and grains of the model material to the thickness of the extracted seam and the size of rock fragments used for mechanical backfilling. A geometric modelling scale of 1:25 was adopted both for the height of the model samples and for the granulometric composition of the crushed rock. The height of the samples is 0.04 m, thus corresponds to a seam thickness of 1.0 m.

As the source material, sandy-clay shale with an in-situ density of 2438 kg/m$^3$ and a bulk density of 1350 kg/m$^3$ was used. The fraction size of the backfill mass in mine conditions was taken as 0.1–150 mm, with $D_{90}$ = 120 mm. The same rock, crushed to a fraction size of 0.1–5 mm, which also corresponds to the 1:25 scale, was used as the model material. Sieve analysis data for the crushed rock for the experimental samples are presented in Table 1 and Fig. 1.

The crushed rock is poorly graded (coefficient of uniformity $C_u = D_{60}/D_{10} = 2.96/0.494 = 6 > 4$). The grain-size distribution is well-graded (coefficient of curvature $C_c = D_{30}^2/(D_{10}D_{60}) = 1.61^2/(0.494 \cdot 2.96) = 1.78$ is within 1–3), and the material is well structured. $D_{90}$ = 4.5 mm.

**Table 1**

Sieve analysis data of crushed rock for experimental models

| Fraction size, mm | % of total volume | | | | | | | Bulk density, $\rho_b$, kg/m$^3$ | Poisson's ratio, $\nu$ |
|---|---|---|---|---|---|---|---|---|---|
| | > 5 | 4–5 | 3–4 | 2–3 | 1–2 | 0.1–1 | < 0.1 | | |
| 0.1–5 | 2 | 16 | 21 | 24 | 18 | 16 | 3 | 1810 | 0.25 |

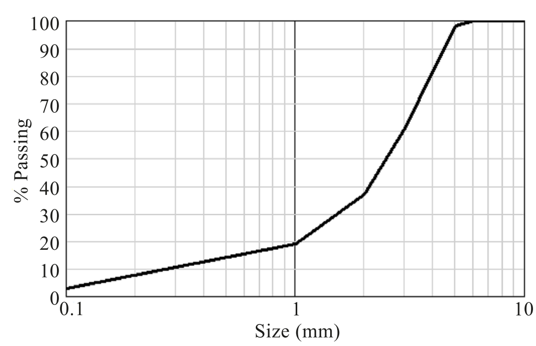


**Fig. 1.** Cumulative grain-size distribution curve of crushed rock

To study the deformation processes in the backfill mass under uniaxial compression with lateral expansion, crushed rock was placed in a fabric shell (experimental models No. 1, 2). The dimensions of the

ISSN-L 2664-9969; E-ISSN 2706-5448

experimental models were: width 0.04 m, length 0.08 m, and initial height 0.04 m. Samples were placed between plates made of sand-cement mixture, simulating the immediate roof and floor strata.

During modeling, the identity of the equilibrium equations in both natural and model conditions was ensured, along with the reproduction of the corresponding deformation conditions. At the same time, to achieve mechanical similarity between the model and the real material, equality of weight parameters was disregarded, since the action of gravity does not affect the deformation processes in the experiment.

Loading conditions were simulated for a depth of 1000 m, which, given an average in-situ rock density of 2400 kg/m$^3$, corresponds to a pressure of 24 MPa. Testing of the models aimed to achieve the same level of loading.

Deformation similarity under such conditions is achieved automatically since dimensionless indicators – relative deformation and compaction coefficient – are studied.

To study deformation processes in the backfill mass without lateral expansion (full backfilling), compressive loading of crushed rock (model No. 3) inside a steel cylinder filled with backfill material was applied. This technique is traditionally used to model backfill masses and the behavior of collapsed rocks in the gob area [14]. The cylinder has a diameter of 0.075 m and a height of 0.075 m.

Characteristics of the experimental models composed of crushed rock are presented in Table 2. The general appearance of the experimental models is shown in Fig. 2.

**Table 2**

Characteristics of experimental models composed of crushed rock

| Loading type | Sample size, m | | | Cross-sectional area, $S$, m$^2$ | Volume of backfill material, $V$, m$^3$ |
|---|---|---|---|---|---|
| | width, $b$ | length, $a$ | height, $h_o$ | | |
| Uniaxial compression with lateral expansion | 0.04 | 0.08 | 0.04 | 0.003 | 0.00012 |
| Compressive loading (compression) | radius $r$ = 0.0375 | | 0.063 | 0.0044 | 0.0027 |

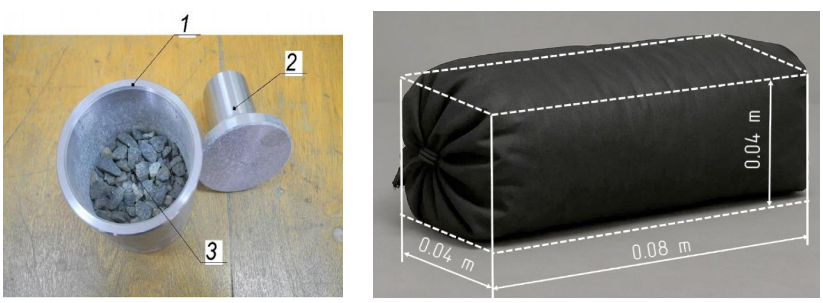


*a* *b*

**Fig. 2.** Appearance of experimental models: *a* – for compressive loading; *b* – for compression with lateral expansion: 1 – steel cylinder, 2 – stamp, 3 – crushed rock

Uniaxial compression of the crushed rock with lateral expansion of the material simulated the loading of the backfill mass under partial backfilling of the gob area. Compressive loading of the crushed rock simulated the loading of the backfill mass under full backfilling of the gob area. The experimental models were placed between metal plates of the P-50 press and subjected to gradual loading. During the tests, the deformation of the model $\Delta h$ (m), and the corresponding load, $F$ (kN), were recorded at each stage of incremental loading.

The relative deformation $\lambda$ of the experimental models was determined by the expression

$$\lambda = \frac{\Delta h}{h_0}. \quad (1)$$

Under loading, the mechanical stress $\sigma$ (Pa or N/m$^2$) is equal to the pressure and is defined as

$$\sigma = \frac{F}{S}. \quad (2)$$

The specific potential energy of deformation or the density of deformation energy $U$ (MJ/m$^3$) of the experimental models was determined by the relation [15]

$$U = \frac{\sigma^2}{2E_d}, \quad (3)$$

where $E_d$ – the deformation modulus, N/m$^2$.

The relative volume change of the material during loading of the models under uniaxial compression with lateral expansion of the crushed rock was determined by the expression

$$\delta V = (1-2\nu)\lambda, \quad (4)$$

where $\nu$ – the Poisson's ratio ($\nu$ = 0.25 [3]).

Under compressive loading conditions, the relative volume change of the backfill material equals the vertical relative deformation

$$\delta V = \frac{\Delta V}{V} = \frac{\Delta h}{h_0} = \lambda. \quad (5)$$

Under uniaxial compression of crushed rock with lateral expansion, the potential energy of deformation can be divided into the energy spent on volume change, $U_v$, and the energy spent on shape change, $U_s$. The ratio of these components of potential energy of deformation under uniform loading depends on the value of Poisson's ratio [15]

$$\frac{U_s}{U_v} = \frac{2(1+\nu)}{1-2\nu}. \quad (6)$$

Under compressive loading conditions, the energy of shape change, $U_s$, can be neglected since the volume change due to compaction predominates.

The compaction coefficient of crushed rock, $k_{comp}$, was determined using the parameter $\Delta V$ under uniaxial compression of experimental models with lateral expansion of the crushed rock. Under compressive loading, $k_{comp}$ was calculated as the ratio of the volume occupied by the crushed rock before compaction to the volume of the material after compaction

$$k_{comp} = \frac{V}{V-\Delta V} = \frac{1}{1-\delta V}. \quad (7)$$

The specific volume change of the backfill material per unit of convergence of lateral rocks, $\Delta V_K$ (m$^{-1}$), during loading of the experimental models was determined by the expression [16]

$$\Delta V_K = \frac{\delta V}{\Delta U_{av}}, \quad (8)$$

where $\Delta U_{av}$ – the average displacement increment.

The average displacement increment was determined as

$$\Delta U_{av} = \frac{\Delta U_i + \Delta U_{i-1}}{2}, \quad (9)$$

where $\Delta U_i$ – the displacement increment, mm.

The displacement increment $\Delta U$ (mm) as the load increases was determined by the expression

$$\Delta U_i = \Delta h_i - \Delta h_{i-1}, \quad (10)$$

where $i$ – the measurement interval number.

This approach allows for the assessment of deformation processes in crushed rock under various compression conditions and the analysis of their impact on the bearing capacity of backfill masses placed in the gob area.

## 3. Results and Discussion

Tables 3, 4 present the experimental data on the loading of models under uniaxial compression of crushed rock with lateral expansion of the backfill material ($\sigma_2 = \sigma_3 = 0$).

Compressive loading represents a special case of triaxial compression with additional boundary conditions that prevent lateral expansion of the material ($\varepsilon_2 = \varepsilon_3 = 0$). Table 5 presents the experimental data of the model loading under compressive loading conditions of the backfill material.

Based on the experimental data presented in Tables 3–5, a comparative analysis of deformation processes in the crushed rock model material was performed.

Fig. 3 shows graphs of the change in relative deformation $\lambda$ of the experimental models as a function of the applied load $F$ (kN) under different compression conditions.

**Table 5**

Experimental data of the loading of the model No. 3 composed of crushed rock under compressive loading conditions

| $F$, kN | $\Delta h$, m | $\lambda$ | $\Delta V$ | $\Delta V_K$, m$^{-1}$ | $\sigma$, MPa | $U$, MJ/m$^3$ | $k_{comp}$ |
|---|---|---|---|---|---|---|---|
| 10 | 0.001 | 0.016 | 0.016 | – | 2.26 | 0.018 | 1.02 |
| 20 | 0.005 | 0.079 | 0.079 | 31.746 | 4.53 | 0.180 | 1.09 |
| 30 | 0.006 | 0.095 | 0.095 | 38.095 | 6.79 | 0.323 | 1.11 |
| 40 | 0.009 | 0.143 | 0.143 | 71.429 | 9.05 | 0.647 | 1.17 |
| 50 | 0.012 | 0.190 | 0.190 | 63.492 | 11.32 | 1.078 | 1.24 |
| 70 | 0.013 | 0.206 | 0.206 | 103.175 | 15.85 | 1.635 | 1.26 |
| 80 | 0.014 | 0.222 | 0.222 | 222.222 | 18.11 | 2.012 | 1.29 |
| 100 | 0.019 | 0.302 | 0.302 | 100.529 | 22.64 | 3.413 | 1.43 |
| 110 | 0.021 | 0.333 | 0.333 | 95.238 | 24.90 | 4.150 | 1.50 |
| 120 | 0.022 | 0.349 | 0.349 | 232.804 | 27.16 | 4.743 | 1.54 |
| 140 | 0.023 | 0.365 | 0.365 | 365.079 | 31.69 | 5.785 | 1.58 |
| 150 | 0.024 | 0.381 | 0.381 | 380.952 | 33.95 | 6.467 | 1.62 |
| 155 | 0.024 | 0.381 | 0.381 | 761.905 | 35.09 | 6.683 | 1.62 |

**Table 3**

Experimental data on the loading of model No. 1, composed of crushed rock of fraction (0.1–5 mm) under uniaxial compression with lateral expansion of the backfill material

| $F$, kN | $\Delta h$, m | $S$, m$^2$ | $\lambda$ | $\Delta V$ | $\Delta V_K$, m$^{-1}$ | $E_d$, MPa | $\sigma$, MPa | $U$, MJ/m$^3$ | $k_{comp}$ |
|---|---|---|---|---|---|---|---|---|---|
| 10 | 0.005 | 0.0032 | 0.125 | 0.063 | – | 24.9 | 3.1 | 0.19 | 1.067 |
| 20 | 0.009 | 0.0034 | 0.225 | 0.113 | 32.143 | 25.9 | 5.8 | 0.65 | 1.127 |
| 30 | 0.015 | 0.0039 | 0.375 | 0.188 | 37.500 | 20.5 | 7.7 | 1.44 | 1.231 |
| 40 | 0.016 | 0.0040 | 0.400 | 0.200 | 57.143 | 25.0 | 10.0 | 2.00 | 1.250 |
| 60 | 0.019 | 0.0044 | 0.475 | 0.238 | 118.750 | 29.0 | 13.8 | 3.27 | 1.311 |
| 70 | 0.021 | 0.0047 | 0.525 | 0.263 | 105.000 | 28.6 | 15.0 | 3.94 | 1.356 |
| 80 | 0.023 | 0.0050 | 0.575 | 0.288 | 143.750 | 27.7 | 15.9 | 4.57 | 1.404 |
| 90 | 0.025 | 0.0055 | 0.625 | 0.313 | 156.250 | 26.2 | 16.4 | 5.11 | 1.455 |
| 100 | 0.026 | 0.0058 | 0.650 | 0.325 | 216.667 | 26.6 | 17.3 | 5.62 | 1.481 |

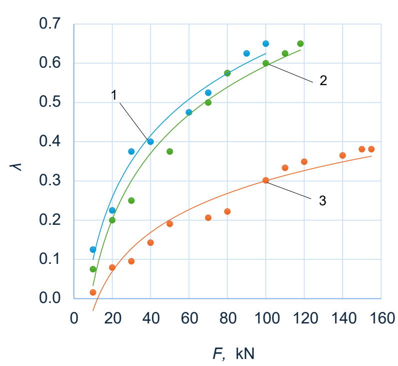


**Fig. 3.** Graphs of relative deformation $\lambda$ versus applied load $F$ (kN): 1, 2 – under uniaxial compression with lateral expansion; 3 – under compressive loading conditions

**Table 4**

Experimental data on the loading of model No. 2 composed of crushed rock of fraction (0.1–5 mm) under uniaxial compression with lateral expansion of the backfill material

| $F$, kN | $\Delta h$, m | $S$, m$^2$ | $\lambda$ | $\Delta V$ | $\Delta V_K$, m$^{-1}$ | $E_d$, MPa | $\sigma$, MPa | $U$, MJ/m$^3$ | $k_{comp}$ |
|---|---|---|---|---|---|---|---|---|---|
| 10 | 0.003 | 0.0031 | 0.075 | 0.038 | – | 42.7 | 3.2 | 0.12 | 1.04 |
| 20 | 0.008 | 0.0034 | 0.200 | 0.100 | 25.000 | 29.6 | 5.9 | 0.59 | 1.11 |
| 30 | 0.01 | 0.0035 | 0.250 | 0.125 | 35.714 | 34.3 | 8.6 | 1.07 | 1.14 |
| 50 | 0.015 | 0.0039 | 0.375 | 0.188 | 53.571 | 34.2 | 12.8 | 2.40 | 1.23 |
| 70 | 0.02 | 0.0045 | 0.500 | 0.250 | 50.000 | 31.1 | 15.6 | 3.89 | 1.33 |
| 80 | 0.023 | 0.0050 | 0.575 | 0.288 | 71.875 | 27.7 | 15.9 | 4.57 | 1.40 |
| 100 | 0.024 | 0.0053 | 0.600 | 0.300 | 150.000 | 31.7 | 19.0 | 5.71 | 1.43 |
| 110 | 0.025 | 0.0055 | 0.625 | 0.313 | 312.500 | 32.0 | 20.0 | 6.25 | 1.45 |
| 118 | 0.026 | 0.0058 | 0.650 | 0.325 | 325.000 | 31.4 | 20.4 | 6.63 | 1.48 |

Under uniaxial compression of crushed rock, the relative deformation of model No. 1 reaches a maximum value of $\lambda = 0.65$ at a load of 100 kN (Fig. 3, curve 1). For model No. 2, the maximum relative deformation $\lambda = 0.65$ was recorded at a load of 118 kN (Fig. 3, curve 2).

Under compressive loading of crushed rock, the maximum relative deformation $\lambda = 0.38$ is reached at a load of 155 kN (Fig. 3, curve 3).

Fig. 4 shows graphs of the influence of mechanical stress $\sigma$ (MPa) on the relative deformation $\lambda$ of the experimental models.

*Model No. 1.* It was recorded that with an increase in stress from 3.1 to 17.3 MPa, the relative deformation increases from 0.12 to 0.65 (Fig. 4, curve 1).

*Model No. 2.* Under conditions where the stress increases from 3.2 to 20.4 MPa, the relative deformation changes from 0.075 to 0.65 (Fig. 4, curve 2).

Under uniaxial compression (models No. 1 and No. 2), the cross-sectional area of the samples changes approximately 2 times (Tables 3, 4).

*Model No. 3.* Under compressive loading of crushed rock with increasing stress from 2.26 to 35.1 MPa, the relative deformation changes from 0.016 to 0.38 (Fig. 4, curve 2).

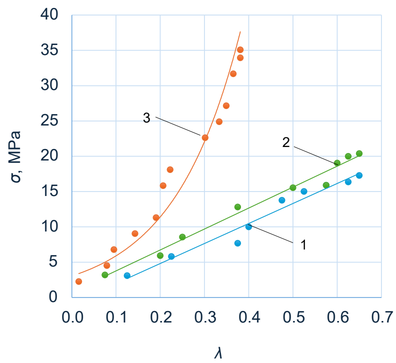


**Fig. 4.** Graphs of the relationship between mechanical stress $\sigma$ (MPa) and relative deformation $\lambda$: 1, 2 – under uniaxial compression with lateral expansion; 3 – under compressive loading conditions

Fig. 5 presents graphs of the change in the specific potential energy of deformation with increasing relative volume change of the backfill material per unit of convergence of the lateral rocks $\Delta V_K$.

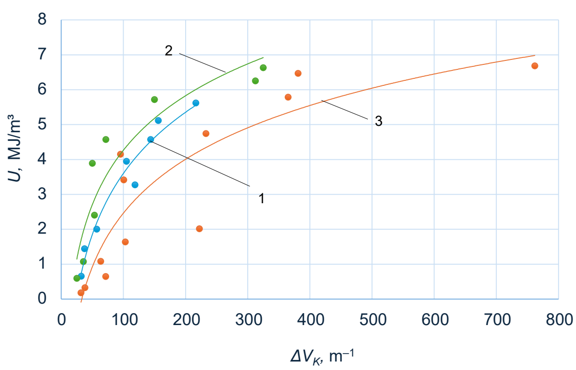


**Fig. 5.** Graph of change in specific potential energy of deformation $U$ (MJ/m$^3$) with relative volume change of the backfill material per unit of convergence of lateral rocks $\Delta V_K$ (m$^{-1}$): 1, 2 – under uniaxial compression with lateral expansion; 3 – under compressive loading conditions

For the experimental models composed of crushed rock under different compression conditions, an exponential growth of the parameter $\Delta V_K$ is recorded with an increase in the specific potential energy of deformation of the backfill material. A logarithmic relationship is established between the studied parameters (the regression equation and the determination coefficients were obtained using the "Regression" tool of the "Data Analysis" package in Microsoft Excel).

For model No. 1, the relationship is of the form

$$U = 2.527\ln(\Delta V_K) - 8.035, \quad (11)$$

with a determination coefficient $R^2 = 0.96$.

For model No. 2, the relationship is of the form

$$U = 2.2513\ln(\Delta V_K) - 6.1, \quad (12)$$

with a determination coefficient $R^2 = 0.88$.

For the compressive loading conditions (model No. 3), the relationship is of the form

$$U = 2.2247\ln(\Delta V_K) - 7.78, \quad (13)$$

with a determination coefficient $R^2 = 0.80$.

Fig. 6 shows the graphs of the average increase in the deformation of the samples and the corresponding change in the specific potential energy of deformation.

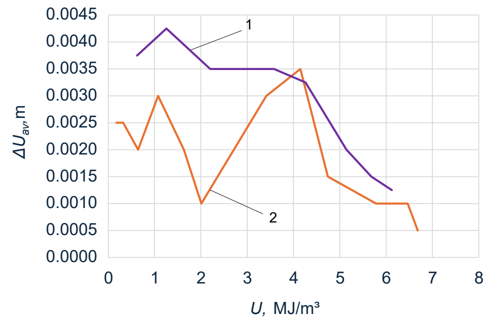


**Fig. 6.** Graph of the change in the average deformation increment of model samples $\Delta U_{av}$ (m) and the corresponding change in the specific potential energy of deformation $U$ (MJ/m$^3$) under the following conditions: 1 – uniaxial compression with lateral expansion (averaged curve based on both experiments); 2 – compressive loading

It was recorded that under uniaxial compression of crushed rock, the area of the sample initially increases due to gradual lateral spreading. During this stage, the deformation increment remains conditionally constant (at the level of 3–4 mm for every 10 kN of applied load) until the specific potential deformation energy reaches about 4–4.5 MJ/m$^3$. With further increase in deformation energy, compaction of the crushed rock core occurs, as indicated by the decrease in the average displacement increment (Fig. 6, curve 1). Under these conditions, most of the deformation energy is spent on changing the shape of the backfill mass.

Under compressive loading of crushed rock, gradual repacking of grains occurs simultaneously with volume reduction of the backfill material – also up to the specific potential deformation energy level of 4–4.5 MJ/m$^3$ (Fig. 6, curve 2). The reduction in the average increase in deformation occurs after the compaction potential of the crushed rock is exhausted, because of grain rearrangement, which leads to an increase in the resistance of the backfill mass. In this case, almost all the deformation energy is spent on changing the volume of the backfill mass.

Fig. 7 shows a graph of the relative volume change of the backfill material per unit of convergence of the lateral rocks as a function of the compaction coefficient of crushed rock.

It was recorded that as the compaction coefficient approaches its maximum values, the parameter $\Delta V_K$ increases progressively. Given that the compaction coefficient has a certain limiting value, the relationship is expected to be hyperbolic, with the asymptote corresponding to the ultimate compaction level.

Based on the results of regression analysis performed in Mathcad, a relationship between the studied parameters was established, expressed by the equation

$$\Delta V_K = \frac{29.51}{1.32 - 0.783k_{comp}}, \quad (14)$$

with a determination coefficient $R^2 = 0.872$.

Similar relationships are observed for the relative volume change of the backfill material per unit of convergence of the lateral rocks, $\Delta V_K$, with increasing relative deformation $\lambda$ of the supporting structures (Fig. 8). At the same time, the expected difference in the deformation is observed between models allowing lateral expansion of the original material and the model under the of its compressive loading conditions.

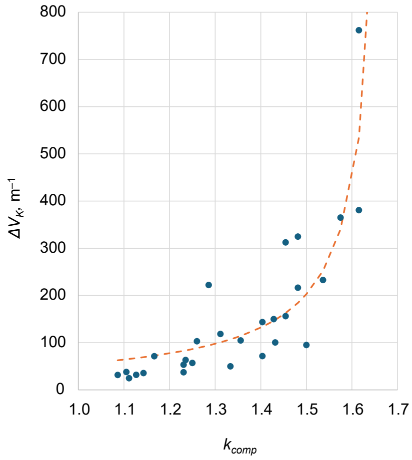


**Fig. 7.** Graph of the relationship between the relative volume change of the backfill material per unit of convergence of the lateral rocks $\Delta V_K$ (m$^{-1}$) and the compaction coefficient of the crushed rock $k_{comp}$

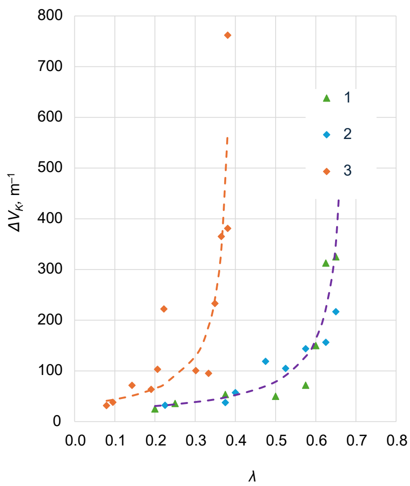


**Fig. 8.** Graph of relative volume change of the backfill mass per unit of convergence of lateral rocks $\Delta V_K$ (m$^{-1}$) from the relative deformation $\lambda$ of the experimental models: 1, 2 – under uniaxial compression with lateral expansion; 3 – under compressive loading conditions

A hyperbolic relationship was established between the studied parameters. For uniaxial compression with lateral expansion (models No. 1, 2), the relationship is of the form

$$\Delta V_K = \frac{22.577}{0.866 - 1.208\lambda}, \quad (15)$$

with a determination coefficient $R^2 = 0.939$.

For compressive loading conditions (model No. 3), the relationship is of the form

$$\Delta V_K = \frac{24.17}{0.732 - 1.811\lambda}, \quad (16)$$

with a determination coefficient $R^2 = 0.888$.

The asymptotic nature of the given dependencies (15)–(17) allows to calculate the limiting values of the compaction coefficient (1.685) and the relative deformation (0.717 and 0.404 for uniaxial and compressive loading, respectively). Using formula (7), the limiting value of the relative volume change of the backfill material can be calculated as

$$\delta V = 1 - \frac{1}{k_{comp}} = 1 - \frac{1}{1.685} = 0.407,$$

or 40.7%, which corresponds to the calculated asymptotic value of the relative deformation (0.404). For comparison, in [17], the maximum shrinkage reserve of the crushed rock backfill mass with a fractional composition of 0–140 mm and a loosening coefficient of 1.7 was determined to be 41.9%, indicating that the results are fully equivalent.

The deformation properties of backfill materials under loading are characterized by the deformation modulus $E_d$, which is the ratio of mechanical stress to the relative deformation caused by it. The average value of the deformation modulus of the backfill material under uniaxial compression ranges between 26–33 MPa. The deformation modulus under compressive loading gradually increases from 57 to 92 MPa. The higher the deformation modulus, the greater the material's resistance to loading. Thus, at comparable compaction coefficients, the difference in the deformation characteristics of the backfill material reaches 2.5–3 times and is essentially determined by the loading conditions.

During uniaxial compression of experimental models, when an increase in the cross-sectional area is recorded (Tables 3, 4), the formation of the bearing core of the backfill material is observed. Irreversible deformations in the backfill material occur at the initial loading stage, when the model expands in the direction perpendicular to the applied load. After reaching the maximum compaction coefficient of the crushed rock $k_{comp}$ = 1.48, longitudinal deformations reflect the shrinkage of the crushed rock and the change in volume of the backfill material. Transverse deformations indicate shape change effects of the maximum compacted volume of the backfill material. The deformation energy of the backfill material under these conditions is mainly spent on shape change ($U_s/U_v$).

The density of deformation energy increases with increasing relative deformation, indicating compaction of the crushed rock within the total volume of the backfill material. The subsequent behavior of the supporting structures depends on the stability of the bearing core of the backfill material (if lateral expansion is possible) or the presence of a compaction reserve.

Under conditions of the compressive loading of the crushed rock, changes in the height and volume of the experimental model occur due to the shrinkage of the backfill material. In the experiment, the maximum compaction coefficient of the crushed rock, 1.62, was reached at a load of 150 kN, which remained unchanged with further loading up to 155 kN, after which loading was stopped. The calculated limiting compaction value allows predicting the maximum shrinkage of the backfill mass and the expected displacements of the roof rocks in the gob-side retained entries.

Under both uniaxial and compressive loading of the backfill material, a redistribution of crushed rock grains occurs; however, in the first case, this is accompanied by changes in both the shape and volume of the backfill mass, while in the second case – only in volume.

Changes in the geometry of backfill masses and the conditions of loading and deformation significantly affect their bearing capacity. The greatest effectiveness of gob backfilling is achieved when continuous backfill masses are formed. In a continuous mass, the crushed rock is subjected to compressive loading. The bearing capacity of the backfill material increases, and the intensity of its deformation decreases due to the reactive resistance of the crushed rock (i. e., increased resistance). With partial backfilling of the gob area, the backfill material operates under uniaxial compression with lateral expansion of the crushed rock, which causes greater shrinkage and lower bearing capacity.

Under real coal seam mining conditions, the backfill material performs the functions of supporting structures. Once the resistance of

ISSN-L 2664-9969; E-ISSN 2706-5448

the backfill masses increases, the movement of the surrounding rock around the mine workings becomes limited, which positively affects the performance of the support system. The greatest effectiveness of gob backfilling is achieved through the formation of continuous backfill masses.

Despite the difference in loading conditions under partial and full backfilling, there are common features in the deformation processes that occur in the backfill masses, which determine their mechanical properties as bearing supports. In particular, this allows making decisions on the feasibility of using full or partial backfilling based on the assessment of expected pressure on the backfill mass and the allowable convergence of the lateral rocks in supported mine roadways, taking into account the nominal yielding capacity of the support system. The research findings can be applied in the extraction of coal seams with moderately to highly collapsible roof rocks. Considering that the degree of additional crushing of the backfill material under pressure depends on its strength properties, the established patterns require verification when applying other types of rocks for backfilling. As for partial backfilling or the protection of mine workings using backfilled walls, it is advisable, based on the established patterns, to study the influence of the geometry and placement of such walls in the gob area on the deformation processes.

## 4. Conclusions

Based on a comparative analysis of deformation processes occurring in the backfill masses composed of crushed rock with a non-uniform grain-size distribution, an assessment of their bearing capacity was carried out, which influences the condition of the surrounding rocks and gob-side retained entries of the coal mine extraction panel.

During the deformation of backfill masses, the work of external forces, which arises due to stress relief in the coal-bearing rock massif, is spent on changing their shape and/or volume. At the same time, the change in the total specific potential energy of deformation of the backfill masses depends on the mechanical properties and exhibits a similar pattern under different compression conditions (uniaxial and confined):

– the density of deformation energy follows a logarithmic relationship with the relative volume change of the backfill material per unit of convergence of the lateral rocks, $\Delta V_K$ ($m^{-1}$);

– the most intensive shrinkage – both with partial and full backfilling – occurs within the deformation energy density range of 4–4.5 $MJ/m^3$;

– the compaction reserve of the backfill material is exhausted when the deformation energy density reaches 5.6–6.7 $MJ/m^3$.

These findings confirm the research hypothesis regarding the presence of common patterns that can be used to predict the bearing capacity of the backfill masses and their behavior under loading.

A hyperbolic relationship between the parameter $\Delta V_K$ and the compaction coefficient and the relative deformation of the crushed rock has been established. The nature of this relationship allows for predicting the ultimate shrinkage of the backfill mass and, accordingly, the expected displacements of the roof rocks in the gob-side retained entries.

The identified patterns can be used to justify technological solutions for roof control that prevent the collapse of lateral rocks and ensure the stability of gob-side retained entries in the extraction panels. For this purpose, similar studies of the deformation properties of the backfill masses with the addition of hardening solutions, as well as options for partial backfilling with artificial restriction of lateral expansion of the backfill material, or in combination with other protective structures. This will further enable the development of measures aimed at improving the efficiency of coal mining and creating safe working conditions for miners in coal mines.

### Conflict of interest

The authors declare that they have no conflict of interest regarding this research, including financial, personal, authorship or other, that could influence the research and its results presented in this article.


### Financing

The research was conducted without financial support.


### Data availability

The manuscript has no related data.

### Use of artificial intelligence

The authors confirm that they did not use artificial intelligence technologies when creating the presented work.

### References


1. Feng, X., Zhang, N., Gong, L., Xue, F., Zheng, X. (2015). Application of a Backfilling Method in Coal Mining to Realise an Ecologically Sensitive "Black Gold" Industry. *Energies, 8 (5)*, 3628–3639. https://doi.org/10.3390/en8053628
2. Jiang, H., Cao, Y., Huang, P., Fang, K., Li, B. (2015). Characterisation of coal-mine waste in solid backfill mining in China. *Mining Technology, 124 (1)*, 56–63. https://doi.org/10.1179/1743286315y.0000000002
3. Yıldız, T. D. (2020). Waste management costs (WMC) of mining companies in Turkey: Can waste recovery help meeting these costs? *Resources Policy, 68*, 101706. https://doi.org/10.1016/j.resourpol.2020.101706
4. Bachurin, L. L., Iordanov, I. V., Simonova, Yu. I., Korol, A. V., Podkopaiev, Ye. S., Kayun, O. P. (2020). Experimental studies of the deformation characteristics of filling massifs. *Technical Engineering, 2 (86)*, 136–149. https://doi.org/10.26642/ten-2020-2(86)-136-149
5. KD 12.01.01.503-2001. *Upravlenie krovlei i kreplenie v ochistnykh zaboiakh na ugolnykh plastakh s uglom padeniia do 35°* (2002). Kyiv: Mintopenergo Ukrainy, DonUGI, 141.
6. Jing, Y., Xu, Y., Bai, J., Li, Y., Li, J. (2025). Mechanism and Control Technology of Lateral Load-Bearing Behavior of a Support System Adjacent to Empty Roadways. *Applied Sciences, 15 (3)*, 1200. https://doi.org/10.3390/app15031200
7. Podkopaiev, S., Gogo, V., Yefremov, I., Kipko, O., Iordanov, I., Simonova, Y. (2019). Phenomena of stability of the coal seam roof with a yielding support. *Mining of Mineral Deposits, 13 (4)*, 28–41. https://doi.org/10.33271/mining13.04.028
8. Krupnik, L. A., Shaposhnik, Yu. N., Shaposhnik, S. N., Tursunbaeva, A. K. (2013). Backfilling technology in Kazakhstan mines. *Journal of Mining Science, 49 (1)*, 82–89. https://doi.org/10.1134/s1062739149010103
9. Zhukov, V. E., Vystorop, V. V., Kolchin, A. M., Grigoriuk, E. V. (1984). *Malootkhodnaia tekhnologiia dobychi uglia*. Kyiv: Tekhnika, 144.
10. Malashkevych, D. S. (2021). *Rozrobka tekhnolohichnykh skhem selektyvnoho vidpratsiuvannia plastiv iz zalyshenniam porody u vyroblenomu prostori (na prykladi shakht Zakhidnoho Donbasu)*. Dnipro: LizunovPres, 189.
11. Shashenko, O. M., Maikherchyk, T., Sdvyzhkova, O. O. (2005). *Heomekhanichni protsesy u porodnykh masyvakh*. Dnipropetrovsk: Natsionalnyi hirnychyi universytet, 319.
12. Kline, S. J. (1986). *Similitude and Approximation Theory*. Springer Berlin Heidelberg, 229. https://doi.org/10.1007/978-3-642-61638-9
13. Shashenko, O. M., Pustovoitenko, V. P., Sdvyzhkova, O. O. (2016). *Heomekhanika*. Kyiv: Novyi druk, 528.
14. Pappas, D. M., Mark, C. (1993). *Behavior of simulated longwall gob material (Report of Investigations No. 9458)*. U.S. Bureau of Mines.
15. Sadd, M. H. (2009). *Elasticity*. Elsevier. https://doi.org/10.1016/B978-0-12-374446-3.X0001-6
16. Chepiga, D., Polii, D., Podkopaiev, S., Bachurin, L., Bielikov, A., Slashchov, I. et al. (2025). Evaluating the stiffness of a cast strip for protecting a prepara-

tory mine working. *Eastern-European Journal of Enterprise Technologies, 2 (1 (134))*, 40–50. https://doi.org/10.15587/1729-4061.2025.324548

17. Petlovanyi, M., Malashkevych, D., Sai, K., Bulat, I., Popovych, V. (2021). Granulometric composition research of mine rocks as a material for backfilling the mined-out area in coal mines. *Mining of Mineral Deposits, 15 (4)*, 122–129. https://doi.org/10.33271/mining15.04.122

***Oleksandr Tkachuk,** PhD, Chief Engineer, Structural Unit "Elektroremont" of PJSC "Donbasenergo", Mykolaivka, Donetsk region, Ukraine, ORCID: https://orcid.org/0000-0002-3129-2275*

✉***Daria Chepiga,** PhD, Department of Mining Management and Labour Protection, Donetsk National Technical University, Drohobych, Ukraine, ORCID: https://orcid.org/0000-0002-3331-9128, e-mail: daria.chepiha@donntu.edu.ua*

***Leonid Bachurin,** PhD, Department of Mining Management and Labour Protection, Donetsk National Technical University, Drohobych, Ukraine, ORCID: https://orcid.org/0000-0003-2513-7284*

***Serhii Podkopaiev,** Doctor of Technical Sciences, Department of Civil Security, Lutsk National Technical University, Lutsk, Ukraine, ORCID: https://orcid.org/0009-0002-6051-4719*

***Yaroslava Bachurina,** Department of Mining Management and Labour Protection, Donetsk National Technical University, Drohobych, Ukraine, ORCID: https://orcid.org/0000-0001-6964-040X*

***Yevgen Podkopayev,** PhD, LLC MS YELTEKO, Kostyantynivka, Ukraine, ORCID: https://orcid.org/0009-0003-2217-3017*

***Mykola Rudynets,** PhD, Department of Civil Security, Lutsk National Technical University, Lutsk, Ukraine, ORCID: https://orcid.org/0000-0002-0793-5963*

***Olena Visyn,** PhD, Department of Civil Security, Lutsk National Technical University, Lutsk, Ukraine, ORCID: https://orcid.org/0000-0003-2361-6708*

✉*Corresponding author*